

# The reconstruction of tachyon inflationary potentials

Qin Fei,<sup>1</sup> Yungui Gong,<sup>1,\*</sup> Jiong Lin,<sup>1</sup> and Zhu Yi<sup>1,†</sup>

<sup>1</sup>*School of Physics, Huazhong University of Science  
and Technology, Wuhan, Hubei 430074, China*

## Abstract

We derive a lower bound on the field excursion for the tachyon inflation, which is determined by the amplitude of the scalar perturbation and the number of  $e$ -folds before the end of inflation. Using the relation between the observables like  $n_s$  and  $r$  with the slow-roll parameters, we reconstruct three classes of tachyon potentials. The model parameters are determined from the observations before the potentials are reconstructed, and the observations prefer the concave potential. We also discuss the constraints from the reheating phase preceding the radiation domination for the three classes of models by assuming the equation of state parameter  $w_{re}$  during reheating is a constant. Depending on the model parameters and the value of  $w_{re}$ , the constraints on  $N_{re}$  and  $T_{re}$  are different. As  $n_s$  increases, the allowed reheating epoch becomes longer for  $w_{re} = -1/3, 0$  and  $1/6$  while the allowed reheating epoch becomes shorter for  $w_{re} = 2/3$ .

---

\* yggong@mail.hust.edu.cn

† yizhu92@hust.edu.cn

## I. INTRODUCTION

Inflation not only provides the solution to the monopole, horizon and flatness problems, but also provides the seeds for the large scale structure of the Universe. The inflationary phase is usually driven by the potential or vacuum energy of a scalar field called the inflaton with a flat potential. Motivated by string theory, tachyon with the effective Dirac-Born-Infeld action is an interesting scalar field [1–4]. Tachyon inflation also provides the almost scale invariant power spectrum [5–7]. To compare inflationary models with the observations, we need to calculate the observables  $n_s$  and  $r$  for a pivotal scale  $k_*$ , and the results are usually expressed in terms of the number of  $e$ -folds  $N_*$  before the end of inflation at the horizon exit of the pivotal scale. For example, the chaotic inflation with the power law potential  $\phi^p$  gives  $n_s = 1 - (p + 2)/(2N_*)$  and  $r = 4p/N_*$  [8], the Starobinsky model gives  $n_s = 1 - 2/N_*$  and  $r = 12/N_*^2$  [9] which is consistent with the Planck 2015 results  $n_s = 0.9645 \pm 0.0049$  and  $r_{0.002} < 0.10$  [10]. Therefore, we can parameterize the observables or the slow-roll parameters with  $N$  for inflationary models [11, 12]. Furthermore, by parameterizing the slow-roll parameters or the observable  $n_s$  with  $N$ , we can constrain the model parameters easily and reconstruct the inflationary potentials [12–33]. The reconstruction method was also applied to tachyon inflation by parameterizing the slow-roll parameter  $\epsilon$  or equivalently  $r$  with  $N$  [34].

In addition to the constraints on  $n_s$  and  $r$ , it was proposed that the reheating phase preceding the radiation domination may provide further constraints on inflationary models [35]. Assuming that the effective equation of state parameter  $w_{re}$  is a constant, we can relate the total number of  $e$ -folds during reheating with  $N_*$  and the energy scale at the end of inflation [35–40]. In this paper, we use the reconstruction method by assuming either constant or simple inverse power law parametrization to reconstruct tachyon potentials and discuss additional constraints from reheating.

The paper is organized as follows. In section II, we review the tachyon inflation and the reconstruction method. The lower bound on the field excursion are derived, and the relation between the reconstruction method and the generalized  $\beta$ -function method is also discussed. In section III, we reconstruct the classes of potentials for the constant  $\eta_V$ , the simple parametrization  $n_s = 1 - p/(N + A)$  and the inverse power-law parametrization  $r = 16\gamma/(N + \alpha)^\beta$ . By assuming that the equation of state parameter  $w_{re}$  during reheating

is a constant, we discuss the constraints on reheating for the three models in section IV, the paper is concluded in section V.

## II. TACHYON INFLATION

The tachyon action is

$$S_T = - \int d^4x \sqrt{-g} V(T) \sqrt{1 + g^{\mu\nu} \partial_\mu T \partial_\nu T}. \quad (1)$$

Applying the Arnowitt-Deser-Misner (ADM) metric [41],

$$ds^2 = -\mathcal{N}^2 dt^2 + h_{ij} (dx^i + N^i dt) (dx^j + N^j dt), \quad (2)$$

the gravitational and tachyon action becomes

$$S = \int d^4x \mathcal{N} \sqrt{h} \left\{ \frac{1}{2} \left[ {}^{(3)}R + \frac{1}{\mathcal{N}^2} (E^{ij} E_{ij} - E^2) \right] - V \left( 1 - \frac{\dot{T}^2}{\mathcal{N}^2} \right)^{\frac{1}{2}} \right\}, \quad (3)$$

where  $\mathcal{N}$  and  $N^i$  are the lapse and the shift functions, respectively, all the spatial indices are raised and lowered by the metric  $h_{ij}$  for the three dimensional space,  $\dot{T} = dT/dt$ ,

$$E_{ij} = \frac{1}{2} \left( \dot{h}_{ij} - \nabla_i N_j - \nabla_j N_i \right), \quad (4)$$

$E = h^{ij} E_{ij}$ , the extrinsic curvature  $K_{ij} = E_{ij}/\mathcal{N}$ , and the covariant derivative is with respect to the three dimensional spatial metric  $h_{ij}$ . Note that we take  $M_{pl} = 1/\sqrt{8\pi G} = 1$ . Since the lapse and shift functions  $\mathcal{N}$  and  $N_i$  contain no time derivative, the variations with respect to them give the corresponding Hamiltonian and momentum constraints,

$$\nabla_i \left[ \frac{1}{\mathcal{N}} (E_j^i - h_{ij} E) \right] = 0, \quad (5)$$

$${}^{(3)}R - \frac{1}{\mathcal{N}^2} (E^{ij} E_{ij} - E^2) - 2V \left( 1 - \frac{\dot{T}^2}{\mathcal{N}^2} \right)^{-\frac{1}{2}} = 0. \quad (6)$$

For the homogeneous and isotropic background,  $\mathcal{N} = 1$ ,  $N_i = 0$  and  $h_{ij} = a^2 \delta_{ij}$ , the Hamiltonian constraint (6) becomes the Friedmann equation

$$H^2 = \frac{1}{3} \frac{V}{\sqrt{1 - \dot{T}^2}}, \quad (7)$$

and the momentum constraint satisfies automatically. The energy density and the equation of state for the tachyon field are

$$\rho = \frac{V}{\sqrt{1 - \dot{T}^2}}, \quad (8)$$

$$w = \frac{p}{\rho} = \dot{T}^2 - 1. \quad (9)$$

The equation of motion for the tachyon field is

$$\frac{\ddot{T}}{1 - \dot{T}^2} + 3H\dot{T} + \frac{V_{,T}}{V} = 0, \quad (10)$$

where  $V_{,T} = dV/dT$ . Combining Eqs. (7) and (10), we get

$$\dot{H} = -\frac{3}{2}H^2\dot{T}^2. \quad (11)$$

### A. slow-roll inflation

From Eq. (11), we get

$$\frac{\ddot{a}}{a} = \dot{H} + H^2 = H^2 \left( 1 - \frac{3}{2}\dot{T}^2 \right). \quad (12)$$

The condition for inflation  $\ddot{a} > 0$  requires  $\dot{T}^2 < 2/3$ . If the tachyon field satisfies the slow-roll conditions

$$\dot{T}^2 \ll 1, \quad (13)$$

$$\ddot{T} \ll 3H\dot{T}, \quad (14)$$

then the background equation during inflation is

$$H^2 \approx \frac{V}{3}, \quad (15)$$

$$3H\dot{T} \approx -V_{,T}/V. \quad (16)$$

By using the number of  $e$ -folds  $N(t) = \ln(a_e/a)$  before the end of inflation,

$$N(t) = \int_t^{t_e} H(t)dt, \quad (17)$$

we introduce the horizon-flow slow-roll parameters [42]

$$\epsilon_0 = \frac{H_*}{H}, \quad (18)$$

$$\epsilon_{i+1} = -\frac{d \ln |\epsilon_i|}{dN}, \quad (19)$$

where the subscript  $e$  denotes the end of inflation, the subscript  $*$  denotes the horizon crossing and we choose  $H_*$  as the Hubble parameter at the horizon crossing for a particular scale, for example,  $k_* = 0.002 \text{ Mpc}^{-1}$ . For the tachyon field, the first two slow-roll parameters are [7]

$$\epsilon = \epsilon_1 = -\frac{\dot{H}}{H^2} = \frac{3}{2}\dot{T}^2 \approx \frac{1}{2}\frac{V_{,T}^2}{V^3}, \quad (20)$$

$$\eta = \epsilon_2 = 2\frac{\ddot{T}}{H\dot{T}} \approx -2\frac{V_{,TT}}{V^2} + 3\frac{V_{,T}^2}{V^3}. \quad (21)$$

From Eqs. (17) and (20), we get

$$N(T) = \pm \sqrt{\frac{3}{2}} \int_T^{T_e} \frac{H}{\sqrt{\epsilon}} dT \approx \int_{T_e}^T \frac{V^2}{V_{,T}} dT, \quad (22)$$

where the  $\pm$  sign is the same as the sign of  $\dot{T}$ .

## B. Perturbations

For convenience, we choose the flat gauge,

$$\begin{aligned} \delta T(x, t) &= 0, \quad \mathcal{N} = 1 + N_1, \quad N_i = \partial_i \psi + N_i^T, \\ h_{ij} &= a^2 \left( (1 + 2\zeta + 2\zeta^2) \delta_{ij} + \gamma_{ij} + \frac{1}{2} \gamma_{il} \gamma_{lj} \right), \end{aligned} \quad (23)$$

where  $\partial^i N_i^T = 0$ ,  $\zeta$  and  $\gamma_{ij}$  denote the scalar and tensor fluctuations respectively, the tensor perturbation satisfies  $\partial_i \gamma^{ij} = 0$  and  $h^{ij} \gamma_{ij} = 0$ . Note that  $N_1$ ,  $\psi$ ,  $N_i^T$ ,  $\zeta$  and  $\gamma_{ij}$  are first order quantities. Substituting Eq. (23) into the momentum constraint (5) and the Hamiltonian constraint (6), to the first order, we get the solution  $N_i^T = 0$  and

$$\begin{aligned} N_1 &= \frac{\dot{\zeta}}{H}, \\ \psi &= -\frac{\zeta}{a^2 H} + \chi, \\ \nabla^2 \chi &= \frac{3}{2} \frac{\dot{T}^2}{1 - \dot{T}^2} \dot{\zeta}. \end{aligned} \quad (24)$$

Combining the solution (24) with the background equations (7), (10) and (11), to the second order of perturbation, the action (3) for the scalar perturbation becomes

$$S = -\frac{3}{2} \int d^4x \left[ a \dot{T}^2 (\partial_i \zeta)^2 - a^3 \frac{\dot{T}^2}{1 - \dot{T}^2} \dot{\zeta}^2 \right]. \quad (25)$$

Using the canonically normalized field  $v = z\zeta$ , where

$$z = \frac{\sqrt{3}a\dot{T}}{\sqrt{1 - \dot{T}^2}}, \quad (26)$$

the action (25) becomes

$$S = \int d^3x d\tau \frac{1}{2} \left[ v'^2 - c_s^2 (\partial_i v)^2 + \frac{z''}{z} v^2 \right], \quad (27)$$

where the prime denotes the derivative with respect to the conformal time  $\tau = \int dt/a$ , and the effective sound speed is  $c_s^2 = 1 - \dot{T}^2$  [5]. In terms of the slow-roll parameters, we get [7]

$$\frac{z''}{z} \approx a^2 H^2 (2 - \epsilon + \frac{3}{2}\eta). \quad (28)$$

To discuss the quantum fluctuations, we define the operator

$$\hat{v}(\tau, \vec{x}) = \int \frac{d^3k}{(2\pi)^3} \left[ v_k(\tau) \hat{a}_k e^{i\vec{k}\cdot\vec{x}} + v_k^*(\tau) \hat{a}_k^\dagger e^{-i\vec{k}\cdot\vec{x}} \right], \quad (29)$$

where the creation and annihilation operators satisfy the standard commutation relations

$$\begin{aligned} [\hat{a}_k, \hat{a}_{k'}^\dagger] &= (2\pi)^3 \delta^3(\vec{k} - \vec{k}'), \\ [\hat{a}_k, \hat{a}_{k'}] &= [\hat{a}_k^\dagger, \hat{a}_{k'}^\dagger] = 0, \end{aligned} \quad (30)$$

and the mode functions obey the normalization condition

$$v'_k v_k^* - v_k v_{k'}^{*'} = -i. \quad (31)$$

We choose the Bunch-Davis vacuum defined by  $\hat{a}_k|0\rangle = 0$ . Varying the action (27) and using Eq. (28), we obtain the Mukhanov-Sasaki equation for the mode function  $v_k(\tau)$  [7],

$$v_k'' + \left( c_s^2 k^2 - \frac{\nu^2 - 1/4}{\tau^2} \right) v_k = 0, \quad (32)$$

where

$$\nu = \frac{3}{2} + \epsilon + \frac{1}{2}\eta. \quad (33)$$

Solving Eq. (32) with the condition (31), we find that outside the horizon, the scalar perturbation is almost a constant,

$$|\zeta_k| = \frac{|v_k|}{z} = 2^{\nu - \frac{5}{2}} \frac{\Gamma(\nu)}{\Gamma(3/2)} \frac{H(1 - \epsilon)^{\nu - 1/2}}{c_s^{1/2} k^{3/2} \epsilon^{1/2}} \left( \frac{c_s k}{aH} \right)^{\frac{3}{2} - \nu}. \quad (34)$$

Therefore, the power spectrum of the scalar perturbation is [7]

$$P_\zeta = \frac{k^3}{2\pi^2} |\zeta_k|^2 = \left[ 1 - \left( \frac{5}{3} + 2C \right) \epsilon - C\eta \right] \frac{H^2}{8\pi^2\epsilon} \Big|_{c_s k = aH}, \quad (35)$$

where  $C = \gamma + \ln 2 - 2 \approx -0.72$ . The amplitude of the scalar perturbation is

$$A_s = \frac{H^2}{8\pi^2\epsilon} \Big|_{c_s k = aH}. \quad (36)$$

The scalar spectral tilt is [5, 7]

$$n_s - 1 = \frac{d \ln P_\zeta}{d \ln k} \Big|_{c_s k = aH} = -2\epsilon - \eta. \quad (37)$$

For the tensor perturbation, to the second order, the action (3) becomes

$$S = \frac{1}{8} \int d^4x \left[ a^3 (\dot{\gamma}_{ij})^2 - a (\gamma_{ij,k})^2 \right], \quad (38)$$

so the tensor spectrum is [7]

$$P_T = [1 - 2(1 + C)\epsilon] \frac{2H^2}{\pi^2} \Big|_{k = aH}. \quad (39)$$

The tensor spectral tilt is [7]

$$n_T = -2\epsilon[1 + \epsilon + (1 + C)\eta]. \quad (40)$$

The tensor to scalar ratio is [5, 7]

$$r = 16\epsilon \left[ 1 - \frac{1}{3}\epsilon + C\eta \right]. \quad (41)$$

### C. Field excursion

If  $\epsilon$  is a monotonic function and  $H$  decreases during inflation, then from Eqs. (22) and (36), we get

$$N_* \leq \sqrt{\frac{3}{2}} \frac{H_*}{\sqrt{\epsilon(T_*)}} |T_e - T_*| = \sqrt{12\pi^2 A_s} M_{pl} \Delta T. \quad (42)$$

In the last equality, we write out  $M_{pl}$  explicitly. Therefore, similar to the Lyth bound [43, 44], there is a lower bound on the field excursion for the tachyon,

$$M_{pl} \Delta T \geq \frac{N_*}{\sqrt{12\pi^2 A_s}} \approx 1.18 \times 10^5 \left( \frac{N_*}{60} \right), \quad (43)$$

where we use the observational value  $\ln(10^{10} A_s) = 3.094$  [10].

#### D. Summary of the relations

From Eqs. (17) and (20), we get

$$\epsilon = \frac{3}{2}\dot{T}^2 \approx \frac{V_{,N}}{2V}. \quad (44)$$

From Eq. (21), we get

$$\eta = \frac{2\ddot{T}}{H\dot{T}} = -\frac{d \ln \epsilon}{dN}. \quad (45)$$

Substituting Eqs. (44) and (45) into Eq. (37), we get

$$n_s - 1 = -2\epsilon + \frac{d \ln \epsilon}{dN} = \left( \ln \frac{V_{,N}}{V^2} \right)_{,N}. \quad (46)$$

From these relations, we see that once we parameterize one of the observable  $n_s$  and  $r$  or the slow-roll parameters  $\epsilon$  and  $\eta$  by  $N$ , we can derive all other parameters and the potential  $V(N)$ . Additionally, if we use the following relation

$$dT \approx \frac{\sqrt{V_{,N}}}{V} dN, \quad (47)$$

to derive the function  $T(N)$ , then we can reconstruct the potential  $V(T)$ . Alternatively, we can derive  $V(T)$  with the following relation,

$$\frac{dV}{dT} = \frac{dV}{dN} \frac{dN}{dT} = V^{3/2} (2\epsilon)^{1/2}. \quad (48)$$

Therefore, by specifying one of the functions  $\epsilon(N)$ ,  $\eta(N)$ ,  $n_s(N)$ ,  $T(N)$  and  $V(N)$ , we can derive the observable  $n_s(N)$  and  $r(N)$  and reconstruct the potential  $V(T)$  within the observable scales.

#### E. The relation to generalized $\beta$ -function formalism

In the generalized  $\beta$ -function formalism [45–47], the superpotential  $W(T) = -2H(T)$  and the  $\beta$ -function is defined as

$$\beta(T) = -2(-p_{,X})^{-1/2} \frac{W_{,T}}{W}, \quad (49)$$

where  $-p_{,X} = \rho = V(T)/\sqrt{1 - \dot{T}^2}$ . By using the Friedman Eqs. (7) and (10), it can be shown that  $\beta^2(T) = 3\dot{T}^2$ , so

$$\beta(T) = -\sqrt{2\epsilon} \approx -\frac{V_{,T}}{V^{3/2}}. \quad (50)$$

For a given  $\beta$ -function, we can reconstruct the potential  $V(T)$  from the above relation. Alternatively, if we parameterize the slow-roll parameters or the observables by  $N$ , we can derive the  $\beta$ -function.

### III. THE RECONSTRUCTION

The simplest parametrization is the constant parametrization. Let us consider  $\epsilon = r/16$  being a constant first. For this case, we get  $\eta = 0$  from Eq. (45), and  $n_s = 1 - 2\epsilon = 1 - r/8$  from Eq. (46). The result  $r = 8(1 - n_s)$  is excluded by the Planck 2015 observations at the  $3\sigma$  level. If we assume that  $\eta$  is a constant, then from Eq. (45), we get

$$\epsilon = e^{-\eta N}, \quad (51)$$

where we choose the integration constant so that  $\epsilon(N = 0) = 1$ . Plugging the result (51) into Eq. (46), we get

$$n_s = 1 - \frac{r}{8} + \frac{1}{N} \ln \left( \frac{r}{16} \right). \quad (52)$$

The result is also excluded by the Planck 2015 observations at the  $3\sigma$  level. Now let us consider the case that  $n_s$  is a constant. From Eq. (46), we get

$$\epsilon = -\frac{\alpha e^{\alpha N}}{2e^{\alpha N} + \alpha D}, \quad (53)$$

$$V = -V_0 \left[ 1 + \frac{2}{\alpha D} e^{\alpha N} \right]^{-1}, \quad (54)$$

where the constant  $\alpha = n_s - 1$ . The end of inflation  $\epsilon(N = 0) = 1$  gives  $D = -(2 + \alpha)/\alpha$ . The tensor to scalar ratio is

$$r = \frac{16(1 - n_s)}{2 - (1 + n_s)e^{(1-n_s)N}}. \quad (55)$$

This result is again excluded by the Planck 2015 observations at the  $3\sigma$  level.

#### A. The constant slow-roll inflation

Now Let us consider the slow-roll parametrization with constant  $\eta_H$ ,

$$\eta_H = -\frac{\ddot{H}}{2H\dot{H}} = \epsilon + \frac{1}{2} \frac{d \ln \epsilon}{dN}, \quad (56)$$

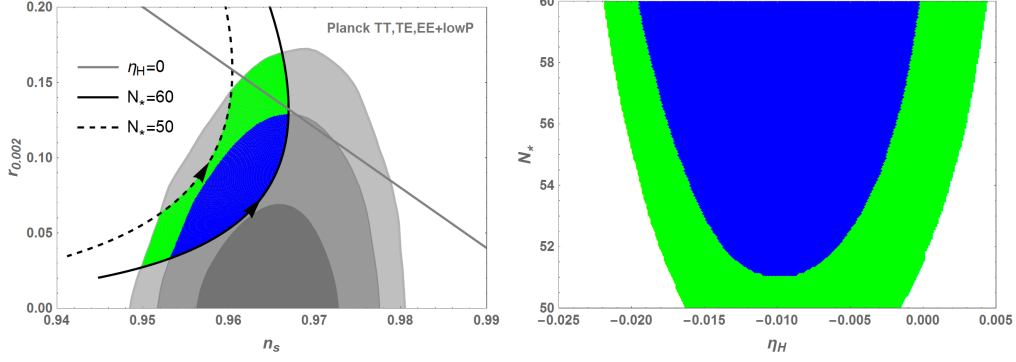


FIG. 1. The marginalized 68%, 95% and 99.8% confidence level contours for  $n_s$  and  $r_{0.002}$  from Planck 2015 data [10] and the observational constraint on  $\eta_H$ . The left panel shows the  $n_s - r$  contours and  $\eta_H$  increases along the arrow direction. The right panel shows the 95% and 99.8% confidence level constraints on  $\eta_H$  and  $N_*$  and they are colored by the blue and green, respectively.

where the constant  $|\eta_H| < 1$ . By imposing the condition  $\epsilon(N = 0) = 1$ , the solution to Eq. (56) is

$$\epsilon = \frac{r}{16} = \frac{\eta_H}{1 + (\eta_H - 1) \exp(-2\eta_H N)}. \quad (57)$$

Substituting the result (57) into Eqs. (46) and (47), we get

$$n_s - 1 = 2\eta_H - \frac{4\eta_H}{1 + (\eta_H - 1) \exp(-2\eta_H N)}, \quad (58)$$

and the reconstructed potential

$$V = 2V_0 \sec^2 \left[ \sqrt{\eta_H V_0} (T - T_0) \right]. \quad (59)$$

Comparing the results (57) and (58) with the Planck 2015 observations [10], we get the constraints on  $\eta_H$  and  $N_*$  and the results are shown in Fig. 1. We see that the constant  $\eta_H$  is not consistent with the observations at the  $1\sigma$  level if  $N_* \leq 60$ .

Next we consider the constant slow-roll parametrization

$$\eta_V = 2 \frac{V_{,TT}}{V^2} \approx \frac{d \ln \epsilon}{dN} + 6\epsilon, \quad (60)$$

where the constant  $|\eta_V| < 1$ . From the definition of  $\eta_V$ , we find that the potential  $V(T)$  takes the form of the Weierstrass function. By imposing the condition  $\epsilon(N = 0) = 1$ , the solution to Eq. (60) is

$$\epsilon = \frac{r}{16} = -\frac{\eta_V}{(6 - \eta_V) e^{-\eta_V N} - 6}. \quad (61)$$

Substituting Eq. (61) into Eq. (46), we get

$$n_s - 1 = \frac{8\eta_V}{(6 - \eta_V)e^{-\eta_V N} - 6} + \eta_V. \quad (62)$$

From Eqs. (61) and (62), we get  $\eta_V = n_s - 1 + r/2$ . Comparing the results (61) and (62) with the Planck 2015 observations [10], we get the constraints on  $\eta_V$  and  $N_*$  and the results are shown in Fig. 2. For  $N_* = 60$ , we get  $-0.0374 < \eta_V < -0.0142$  at the  $1\sigma$  level,  $-0.0435 < \eta_V < -0.0031$  at the  $2\sigma$  level and  $-0.0473 < \eta_V < 0.0067$  at the  $3\sigma$  level. From Fig. 2, we see that  $\eta_V < 0$  is favored at more than  $2\sigma$  confidence level, so the concave potential is preferred. From now on, we call constant  $\eta_V$  as the constant slow-roll inflation.

Substituting Eq. (61) into Eq. (44), we get

$$V(N) = V_0 \left| 6e^{\eta_V N} - 6 + \eta_V \right|^{\frac{1}{3}}, \quad (63)$$

where

$$V_0 = \frac{3\pi^2 A_s r}{2} \left| \frac{8 - 8n_s - r}{(8 - 8n_s - 4r)(7 - n_s - r/2)} \right|^{1/3}. \quad (64)$$

From Eq. (47), we get

$$dT = \frac{2}{\eta_V} \sqrt{\frac{2|\eta_V|}{V_0}} \frac{1}{(6x^2 - 6 + \eta_V)^{2/3}} dx, \quad (65)$$

where  $x = e^{\eta_V N/2}$ . The solution gives the Hypergeometric function

$$T - T_0 = \frac{2}{\eta_V} \sqrt{\frac{2|\eta_V|}{V_0}} \frac{\exp(\eta_V N/2)}{(6 - \eta_V)^{2/3}} {}_2F_1 \left( \frac{1}{2}, \frac{2}{3}; \frac{3}{2}; \frac{6e^{\eta_V N}}{6 - \eta_V} \right). \quad (66)$$

Combining Eqs. (63) and (66), we can obtain the potential  $V(T)$ . If we take  $\eta_V = -0.021$  and  $N_* = 60$ , we get  $n_s = 0.968$ ,  $r = 0.022$  and  $\Delta T = T_* - T_e = 3.66 \times 10^5$ , so the field excursion satisfies the bound (43). By using these parameters, we plot the potential in Fig. 3.

## B. The power law parametrization of $n_s$

The observational data favors  $n_s = 1 - 2/N_*$  with  $N_* = 60$ , so we choose the parametrization

$$n_s = 1 - \frac{p}{N + A}. \quad (67)$$

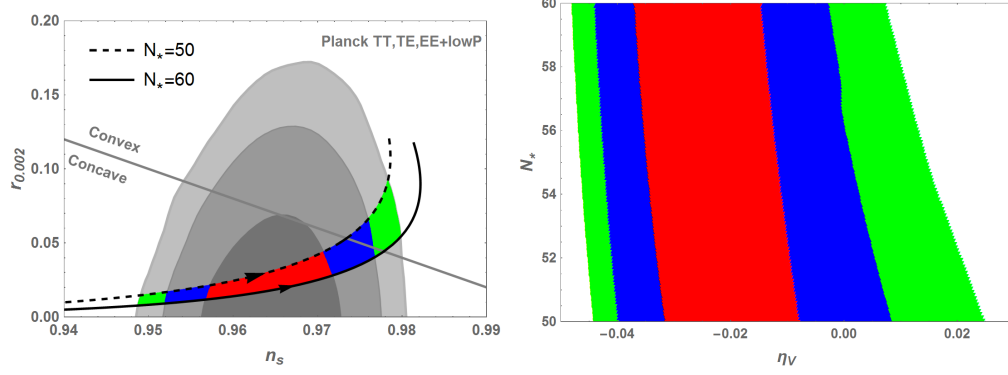


FIG. 2. The marginalized 68%, 95% and 99.8% confidence level contours for  $n_s$  and  $r_{0.002}$  from Planck 2015 data [10] and the observational constraint on  $\eta_V$ . The left panel shows the  $n_s - r$  contours and  $\eta_V$  increases along the arrow direction. The right panel shows the 68%, 95% and 99.8% confidence level constraints on  $\eta_V$  and  $N_*$  and they are colored by the red, blue and green, respectively.

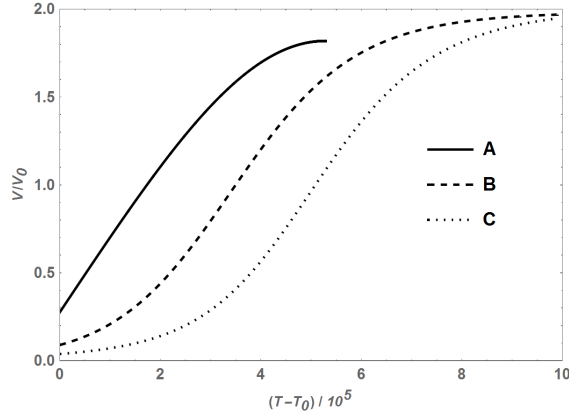


FIG. 3. The reconstructed potentials. The solid line A corresponds to the potential for the constant slow-roll inflation, the dashed line B denotes the potential (75), and the dotted line C denotes the potential from Eq. (95).

From Eq. (46), we get

$$\epsilon(N) = \begin{cases} \frac{p-1}{2(N+A) + 2C(p-1)(N+A)^p}, & p \neq 1, \\ \frac{1}{2(N+A)[C - \ln(N+A)]}, & p = 1, \end{cases} \quad (68)$$

and

$$V(N) = \begin{cases} \frac{\tilde{V}_0(p-1)}{(p-1)C + (N+A)^{1-p}}, & p \neq 1, \\ \frac{\tilde{V}_0}{C - \ln(N+A)}, & p = 1, \end{cases} \quad (69)$$

where  $C$  and  $\tilde{V}_0$  are integration constants.

For convenience, let us consider the case  $p = 1$  first. At the end of inflation,  $N = 0$  and  $\epsilon(N) = 1$ , so  $C = (2A)^{-1} + \ln A$ , and we get

$$n_s = 1 - \frac{1}{N+A}, \quad (70)$$

$$r = \frac{16A}{(N+A)(1 - A \ln[(N+A)/A]^2)}. \quad (71)$$

It is easy to show that the results are excluded by the Planck 2015 observations [10] at the  $3\sigma$  level.

For  $p \neq 1$ , from the condition  $\epsilon(N=0) = 1$ , we get  $p-1-2A = 2C(p-1)A^p$ , so the tensor to scalar ratio are

$$r = \frac{16(p-1)}{2(N+A) + (p-1-2A)(N+A)^p/A^p}. \quad (72)$$

Note that if  $C = 0$ , then  $p = 1 + 2A$  and  $r = 8[N(1 - n_s) - 1]/(N - 1/2)$ . If  $p > 1 + 2A$  with  $A > 0$ , then  $r \sim 1/N^p$ . In particular, for the case  $p = 2$ , we get the familiar  $\alpha$  attractor  $n_s = 1 - 2/N_*$  and  $r = 12\alpha/N_*^2$  for large  $N$  and  $C \neq 0$ . Comparing the results (67) and (72) with the Planck 2015 observations [10], taking  $N_* = 60$ , we get the constraints on  $p$  and  $A$  and the results are shown in Fig. 4. From Fig. 4, we see that the results are similar to those for canonical scalar field [24].

Now we proceed to derive the class of potentials. From Eq. (47), we get

$$dT = \tilde{V}_0^{-1/2}(N+A)^{-\frac{p}{2}}dN. \quad (73)$$

For  $p \neq 1$  and  $p \neq 2$ , we have

$$N(T) + A = \left[ \frac{(2-p)\sqrt{\tilde{V}_0}}{2}(T - T_0) \right]^{\frac{2}{2-p}}. \quad (74)$$

Combining Eqs. (69) and (74), for  $p \neq 1+2A$ ,  $p \neq 1$  and  $p \neq 2$ , we get the inverse power-law potential [7, 48, 49]

$$V(T) = V_0 \left[ 1 + \beta_1(T - T_0)^{\frac{2p-2}{p-2}} \right]^{-1}, \quad (75)$$

where

$$V_0 = \frac{2\tilde{V}_0(p-1)A^p}{p-1-2A}, \quad (76)$$

$$\beta_1 = \frac{2A^p\tilde{V}_0^{(p-1)/(p-2)}}{p-1-2A} \left( \frac{2-p}{2} \right)^{2(p-1)/(p-2)}, \quad (77)$$

and

$$V(T) = (p-1)\tilde{V}_0 \left[ \frac{(2-p)\sqrt{\tilde{V}_0}}{2} (T-T_0) \right]^{2(p-1)/(2-p)}, \quad (78)$$

for  $p = 1 + 2A$ ,  $p \neq 1$  and  $p \neq 2$ . If we take  $p = 1.934$ ,  $A = 0.446$  and  $N_* = 60$ , we get  $n_s = 0.968$ ,  $r = 0.022$ , and  $\Delta T = T_* - T_e = 5.4 \times 10^5$ , so the bound (43) is satisfied. With these model parameters, we plot the potential (75) in Fig. 3.

For  $p = 2$ , we have

$$N(T) + A = \exp \left[ \sqrt{\tilde{V}_0} (T - T_0) \right]. \quad (79)$$

Combining Eqs. (69) and (79), we get the potential for the  $\alpha$  attractor (67) with  $p = 2$

$$V(T) = V_0 \left[ 1 + \beta_2 \exp \left( -\sqrt{\tilde{V}_0} (T - T_0) \right) \right]^{-1}, \quad (80)$$

where  $A \neq 1/2$  and

$$V_0 = \frac{2A^2\tilde{V}_0}{1-2A}, \quad (81)$$

$$\beta_2 = \frac{2A^2}{1-2A}, \quad (82)$$

and

$$V(T) = \tilde{V}_0 \exp \left[ \sqrt{\tilde{V}_0} (T - T_0) \right], \quad (83)$$

for  $A = 1/2$  and  $p = 2$ .

### C. The power-law parametrization of $r$

In this subsection, we consider the parametrization

$$\epsilon = \frac{r}{16} = \frac{\gamma}{(N + \alpha)^\beta}, \quad (84)$$

where  $\gamma = \alpha^\beta$  so that  $\epsilon(N = 0) = 1$ . Substituting the parametrization (84) into Eq. (46), we get

$$n_s - 1 = -2 \left( \frac{\alpha}{N + \alpha} \right)^\beta - \frac{\beta}{N + \alpha}. \quad (85)$$

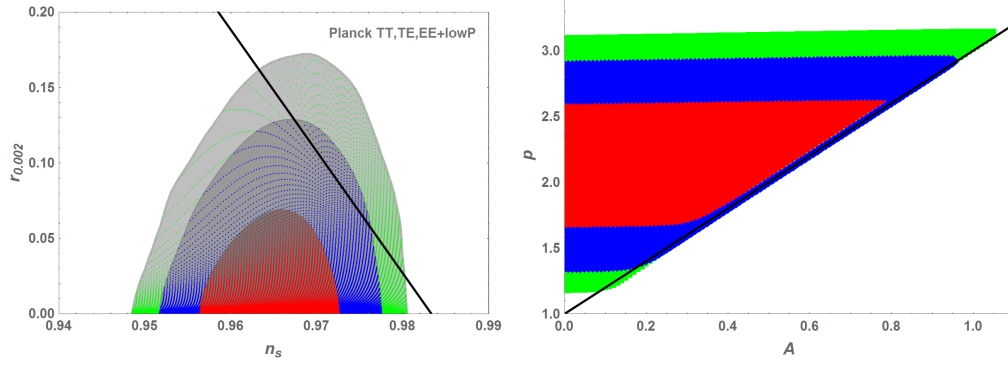


FIG. 4. The marginalized 68%, 95% and 99.8% confidence level contours for  $n_s$  and  $r_{0.002}$  from Planck 2015 data [10] and the theoretical predictions for the parametrization (67) with  $N_* = 60$ . The left panel shows the  $n_s - r$  contours and the right panel shows the constraints on  $p$  and  $A$  for  $N_* = 60$ . The red, blue and green regions correspond to 68%, 95% and 99.8% confidence levels, respectively. The solid black line denotes  $p = 1 + 2A$ .

Comparing the results (84) and (85) with the Planck 2015 observations [10], we get the constraints on  $\alpha$  and  $\beta$  and the results are shown in Fig. 5. Substituting Eq. (84) into Eq. (44), we get

$$V(N) = \tilde{V}_0(N + \alpha)^{2\alpha}, \quad (86)$$

for  $\beta = 1$ , and

$$V = \tilde{V}_0 \exp \left[ \frac{2\gamma}{1 - \beta} (N + \alpha)^{1-\beta} \right], \quad (87)$$

for  $\beta \neq 1$ . So for  $\beta \neq 1$ , combining Eqs. (84) and (87), we get

$$\epsilon = \gamma \left[ \frac{1 - \beta}{2\gamma} \ln \left( \frac{V}{\tilde{V}_0} \right) \right]^{-\frac{\beta}{1-\beta}}. \quad (88)$$

Let us consider the case  $\beta = 1$  first. Substituting Eq. (86) into Eq. (47), we get

$$\frac{dT}{dN} = \sqrt{\frac{2\alpha}{\tilde{V}_0}} (N + \alpha)^{-\alpha - \frac{1}{2}}. \quad (89)$$

If  $\alpha = 1/2$ , then

$$N + \alpha = \exp \left[ \sqrt{\tilde{V}_0} (T - T_0) \right]. \quad (90)$$

Combining Eq. (86) and Eq. (90), we get the exponential potential [34] for  $\beta = 1$  and  $\alpha = 1/2$

$$V = \tilde{V}_0 \exp \left[ \sqrt{\tilde{V}_0} (T - T_0) \right]. \quad (91)$$

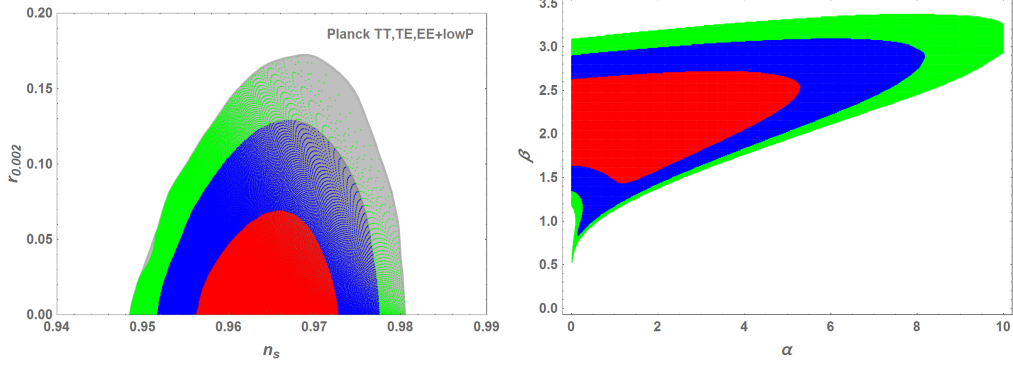


FIG. 5. Same as Fig. 4 but for the parametrization (84). The left panel shows the  $n_s - r$  contours and the right panel shows the constraints on  $\alpha$  and  $\beta$  for  $N_* = 60$ . The red, blue and green regions correspond to 68%, 95% and 99.8% confidence levels, respectively.

If  $\alpha \neq 1/2$ , then

$$N + \alpha = \left[ \sqrt{\frac{\tilde{V}_0}{2\alpha}} \left( \frac{1}{2} - \alpha \right) (T - T_0) \right]^{\frac{2}{1-2\alpha}}. \quad (92)$$

Combining Eq. (86) and Eq. (92), we get the power-law potential [34] for  $\beta = 1$  and  $\alpha \neq 1/2$

$$V = V_0 (T - T_0)^{4\alpha/(1-2\alpha)}, \quad (93)$$

where

$$V_0 = \tilde{V}_0 \left[ \sqrt{\frac{\tilde{V}_0}{2\alpha}} \left( \frac{1}{2} - \alpha \right) \right]^{\frac{4\alpha}{1-2\alpha}}. \quad (94)$$

Now let us discuss the general case  $\beta \neq 1$ . Substituting Eq. (88) into Eq. (48), we get

$$\sqrt{2\gamma} dT = \left[ \frac{1-\beta}{2\gamma} \ln \left( \frac{V}{\tilde{V}_0} \right) \right]^{\frac{\beta}{2(1-\beta)}} \frac{dV}{\sqrt{V^3}}. \quad (95)$$

Although the analytic form for  $V(T)$  is not available, the potential  $V(T)$  can be obtained from Eq. (95) and it is shown in Fig. 3. If we take  $\alpha = 1.588$ ,  $\beta = 1.801$  and  $N_* = 60$ , we get  $n_s = 0.968$ ,  $r = 0.022$  and  $\Delta T = T_* - T_e = 6.93 \times 10^5$ , so the bound (43) is satisfied.

#### IV. REHEATING

The pivotal scale  $k_* = 0.002 \text{Mpc}^{-1}$  is related to the current Hubble horizon as

$$\frac{c_s k_*}{a_0 H_0} = \frac{a_* H_*}{a_0 H_0} = \frac{a_*}{a_e} \frac{a_e}{a_{re}} \frac{a_{re}}{a_0} \frac{H_*}{H_0} = e^{-N_* - N_{re}} \frac{a_{re}}{a_0} \frac{H_*}{H_0}, \quad (96)$$

where  $a_{re}$  denotes the value of the scale factor at the end of reheating,  $N_{re}$  denotes the number of  $e$ -folds during reheating, and we assume that radiation domination begins immediately after the reheating, and reheating begins immediately after inflation. If the equation of state parameter  $w_{re}$  is a constant during reheating, then we have

$$N_{re} = \frac{1}{3(1+w_{re})} \ln \frac{\rho_e}{\rho_{re}}, \quad (97)$$

where  $\rho_{re}$  is related with the temperature  $T_{re}$  as

$$\rho_{re} = \frac{\pi^2}{30} g_{re} T_{re}^4, \quad (98)$$

and  $g_{re}$  is the effective number of relativistic species at reheating. From the entropy conservation, we can express the temperature  $T_{re}$  with the current cosmic microwave background temperature  $T_0 = 2.725K$  through the following relation

$$a_{re}^3 g_{s,re} T_{re}^3 = a_0^3 \left( 2T_0^3 + 6 \times \frac{7}{8} T_{\nu 0}^3 \right), \quad (99)$$

where  $g_{s,re}$  is the effective number of relativistic species for entropy and the current neutrino temperature  $T_{\nu 0} = (4/11)^{1/3} T_0$ . Combining the above results, we get [35, 36]

$$N_{re} = \frac{4}{1-3w_{re}} \left[ -N_* - \ln \frac{\rho_e^{1/4}}{H_*} + \frac{1}{3} \ln \frac{43}{11g_{s,re}} + \frac{1}{4} \ln \frac{\pi^2 g_{re}}{30} - \ln \frac{c_s k_*}{a_0 T_0} \right], \quad (100)$$

$$T_{re} = \exp \left[ -\frac{3N_{re}(1+w_{re})}{4} \right] \left[ \frac{30\rho_e}{\pi^2 g_{re}} \right]^{1/4}. \quad (101)$$

Since  $N_{re}$  and  $T_{re}$  depend on  $g_{re}$  and  $g_{s,re}$  logarithmically, so it is safe to take  $g_{re} = g_{s,re} = 106.75$ . Since at the end of inflation,  $\dot{T}^2 = 2/3$ , so  $\rho_e = \sqrt{3}V_e$ . Using the observational value [10]

$$A_s = H_*^2 / (8\pi^2 \epsilon_*) = 2.2 \times 10^{-9}, \quad (102)$$

we get

$$N_{re} = \frac{4}{1-3w_{re}} \left( 56.94 - N_* - \frac{1}{4} \ln V_e + \frac{1}{2} \ln \epsilon_* \right), \quad (103)$$

$$T_{re} = \exp \left[ -\frac{3N_{re}(1+w_{re})}{4} \right] \left[ \frac{3\sqrt{3}V_e}{10.675\pi^2} \right]^{1/4}. \quad (104)$$

These results (103) and (104) can be used to constrain inflationary models.

For the constant slow-roll inflation (60), at the horizon exit, we have

$$3H_*^2 = V_0 \left| 6e^{\eta_V N_*} - 6 + \eta_V \right|^{1/3}. \quad (105)$$

At the end of inflation,  $V_e = V_0|\eta_V|^{1/3}$ , so

$$V_e = 24\pi^2\epsilon_*A_s \left[ \frac{\eta_V e^{-\eta_V N_*}}{6 - (6 - \eta_V)e^{-\eta_V N_*}} \right]^{1/3}. \quad (106)$$

In deriving the above result, we used the relation  $H_*^2 = 8\pi^2\epsilon_*A_s$ . Substituting Eqs. (61) and (106) into Eqs. (103) and (104), we get

$$N_{re} = \frac{4}{1 - 3w_{re}} \left\{ 60.56 - \left(1 - \frac{\eta_V}{12}\right) N_* + \frac{1}{6} \ln \left[ \frac{\eta_V}{6 - (6 - \eta_V)e^{-\eta_V N_*}} \right] \right\}, \quad (107)$$

$$T_{re} = 0.01 \left[ \frac{\eta_V}{6 - (6 - \eta_V)e^{-\eta_V N_*}} \right]^{1/3} \exp \left[ -\frac{3N_{re}(1 + w_{re})}{4} - \frac{\eta_V N_*}{12} \right]. \quad (108)$$

By choosing different values for  $\eta_V$  and  $w_{re}$ , we calculate  $n_s$ ,  $N_{re}$  and  $T_{re}$  by varying  $N_*$ , and the results are shown in Fig. 6. The parameter  $\eta_V$  is chosen as  $\eta_V = -0.03$ ,  $-0.025$  and  $-0.02$  respectively from the left to right in Fig. 6, the gray region corresponds to the  $1\sigma$  Planck constraint  $n_s = 0.9645 \pm 0.0049$  [10], and the  $1\sigma$  constraint on  $N_*$  for the chosen value of  $\eta_V$  is also shown. The black, red, blue and green lines denote  $w_{re} = -1/3$ ,  $0$ ,  $1/6$  and  $2/3$ , respectively. The horizontal gray solid and dashed lines in lower panels correspond to the electroweak scale  $T_{EW} \sim 100$  GeV and the big bang nucleosynthesis scale  $T_{BBN} \sim 10$  MeV, respectively. From Fig. 6, we see that depending on the model parameter  $\eta_V$  and the reheating physics (the value of  $w_{re}$ ), the constraints on  $N_{re}$  and  $T_{re}$  are different. As  $\eta_V$  becomes larger,  $n_s$  increases, the allowed reheating epoch becomes longer for  $w_{re} = -1/3$ ,  $0$  and  $1/6$  while the allowed reheating epoch becomes shorter for  $w_{re} = 2/3$ . For  $-0.03 < \eta_V < -0.02$ , reheating with  $-1/3 \leq w_{re} \leq 2/3$  are all consistent with the observations. Around the central value  $n_s = 0.965$ ,  $\eta_V = -0.025$  and  $N_* = 60$ ,  $w_{re} = 1/6$  can have a prolonged reheating epoch and  $N_{re}$  can be larger than 70.

For the model (67), we consider the case  $p > 1$  and  $p \neq 1 + 2A$ . Substituting Eqs. (68) and (69) into Eqs. (103) and (104), we get

$$N_{re} = \frac{4}{1 - 3w_{re}} \left\{ 60.38 + \frac{1}{4} \ln [C(p - 1)^2 + (p - 1)A^{1-p}] - N_* - \frac{p}{4} \ln (N_* + A) - \frac{1}{2} \ln [(N_* + A)^{1-p} + C(p - 1)] \right\}, \quad (109)$$

$$T_{re} = 0.01 (N_* + A)^{-p/4} \left[ \frac{p - 1}{A^{1-p} + (p - 1)C} \right]^{1/4} \exp \left[ -\frac{3N_{re}(1 + w_{re})}{4} \right]. \quad (110)$$

By choosing different values of  $p$ ,  $A$ ,  $N_*$  and  $w_{re}$ , we calculate  $n_s$ ,  $N_{re}$  and  $T_{re}$  from Eqs. (62), (109) and (110), and the results are shown in Fig. 7. From Fig. 7, we see that depending

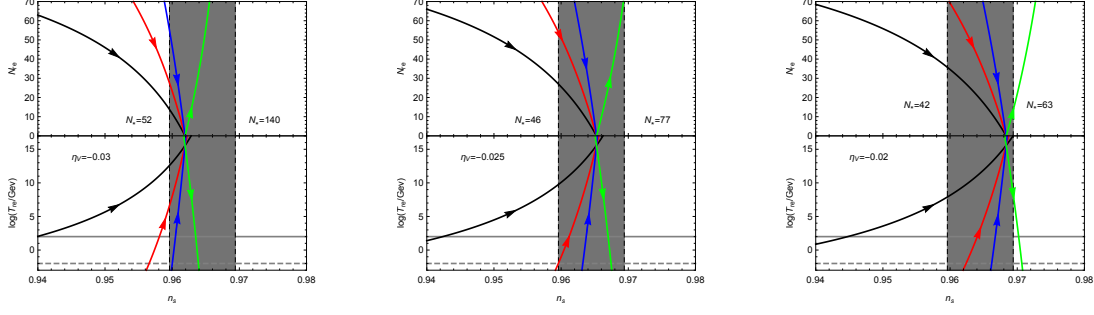


FIG. 6.  $N_{re}$  (upper panels) versus  $n_s$  as determined from (62) and (107), and  $T_{re}$  (lower panels) versus  $n_s$  as determined from (62) and (108) for the constant slow-roll inflation. From the left to right, the parameter  $\eta_V$  is chosen as  $\eta_V = -0.03$ ,  $-0.025$  and  $-0.02$ , respectively. The gray band corresponds to the  $1\sigma$  Planck constraint  $n_s = 0.9645 \pm 0.0049$  [10], and the  $1\sigma$  constraint on  $N_*$  is also given. In each panel, the black, red, blue and green lines denote  $w_{re} = -1/3$ ,  $0$ ,  $1/6$  and  $2/3$ , respectively, and the arrow indicates that  $N_*$  increases along the line. The horizontal gray solid and dashed lines in lower panels correspond to the electroweak scale  $T_{EW} \sim 100$  GeV and the big bang nucleosynthesis scale  $T_{BBN} \sim 10$  MeV, respectively.

on the model parameters  $p$  and  $A$  and the value of  $w_{re}$ , the constraints on  $N_{re}$  and  $T_{re}$  are different, but the parameter  $A$  has little impact on the reheating phase. For the parameters  $p$  and  $A$  that makes  $n_s$  consistent with the observation, reheating with  $-1/3 \leq w_{re} \leq 2/3$  are all consistent with the observations. As  $n_s$  becomes larger, the allowed reheating epoch becomes longer for  $w_{re} = -1/3$ ,  $0$  and  $1/6$  while the allowed reheating epoch becomes shorter for  $w_{re} = 2/3$ .

For the model (84), we consider the case  $\beta \neq 1$ , Substituting Eqs. (84) and (87) into Eqs. (103) and (104), we obtain

$$N_{re} = \frac{4}{1 - 3w_{re}} \left[ 60.56 + \frac{\alpha}{2(\beta - 1)} - N_* - \frac{\alpha}{2(\beta - 1)} \left( \frac{N_* + \alpha}{\alpha} \right)^{1-\beta} - \frac{\beta}{4} \ln \left( \frac{N_* + \alpha}{\alpha} \right) \right], \quad (111)$$

$$T_{re} = 0.01 \left( \frac{\alpha}{N_* + \alpha} \right)^{\beta/4} \exp \left[ -\frac{3N_{re}(1 + w_{re})}{4} + \frac{\alpha}{2(1 - \beta)} \left( 1 - \left( \frac{N_* + \alpha}{\alpha} \right)^{1-\beta} \right) \right]. \quad (112)$$

By choosing different values of  $\alpha$ ,  $\beta$ ,  $N_*$  and  $w_{re}$ , we calculate  $n_s$ ,  $N_{re}$  and  $T_{re}$  from Eqs. (62), (111) and (112), and the results are shown in Fig. 8. It is obvious that depending on the model parameters  $\alpha$  and  $\beta$  and the value of  $w_{re}$ , the constraints on  $N_{re}$  and  $T_{re}$  are

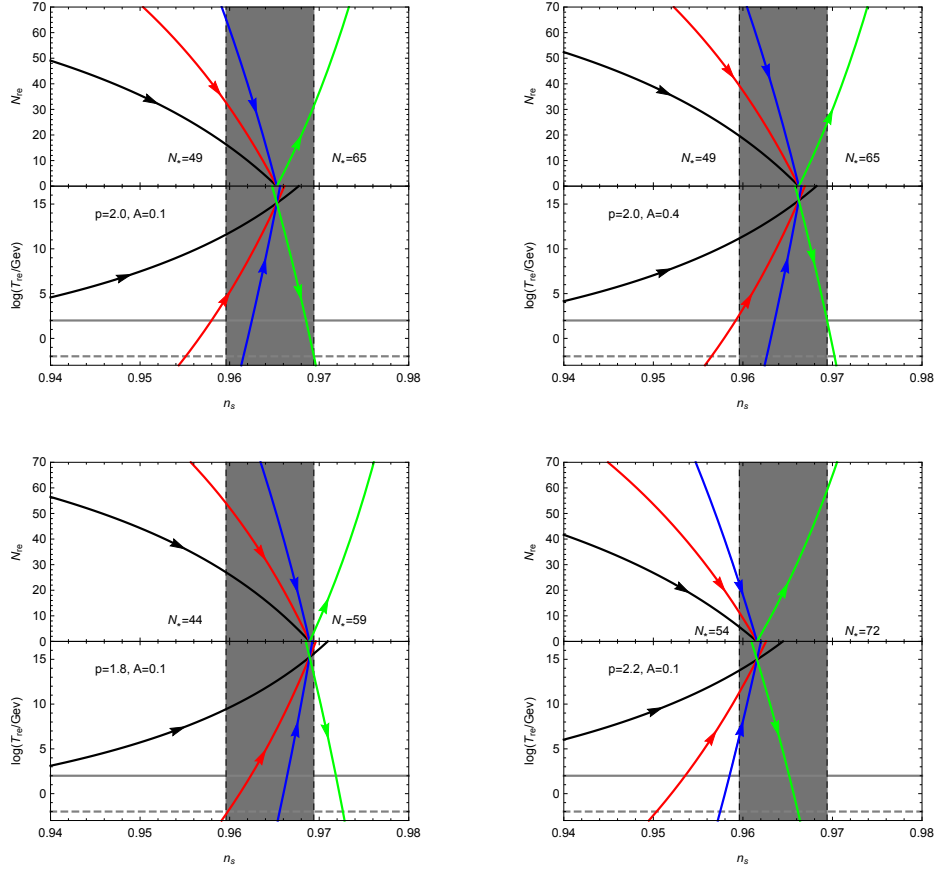


FIG. 7. Same as Fig. 6 but for the model (67), the values of the model parameters  $p$  and  $A$  are indicated in each panel.

different, but the parameter  $\alpha$  has little impact on the reheating phase. For the parameters  $\alpha$  and  $\beta$  that makes  $n_s$  consistent with the observation, reheating with  $-1/3 \leq w_{re} \leq 2/3$  are all consistent with the observations. As  $n_s$  becomes larger, the allowed reheating epoch becomes longer for  $w_{re} = -1/3, 0$  and  $1/6$  while the allowed reheating epoch becomes shorter for  $w_{re} = 2/3$ .

## V. CONCLUSIONS AND DISCUSSIONS

Similar to the usual inflation with canonical scalar field, there is also a lower bound on the field excursion for the tachyon inflation, but the lower bound for the tachyon field depends on  $A_s$  and  $N_*$ . Using the observational value  $\ln(10^{10}A_s) = 3.094$  [10], we derive the lower bound  $\Delta T \geq 1.18 \times 10^5$  normalized with the reduced Planck mass  $M_{pl}$  for  $N_* = 60$ , and the bound are supported by the three models discussed in this work. Since the  $\beta$ -function

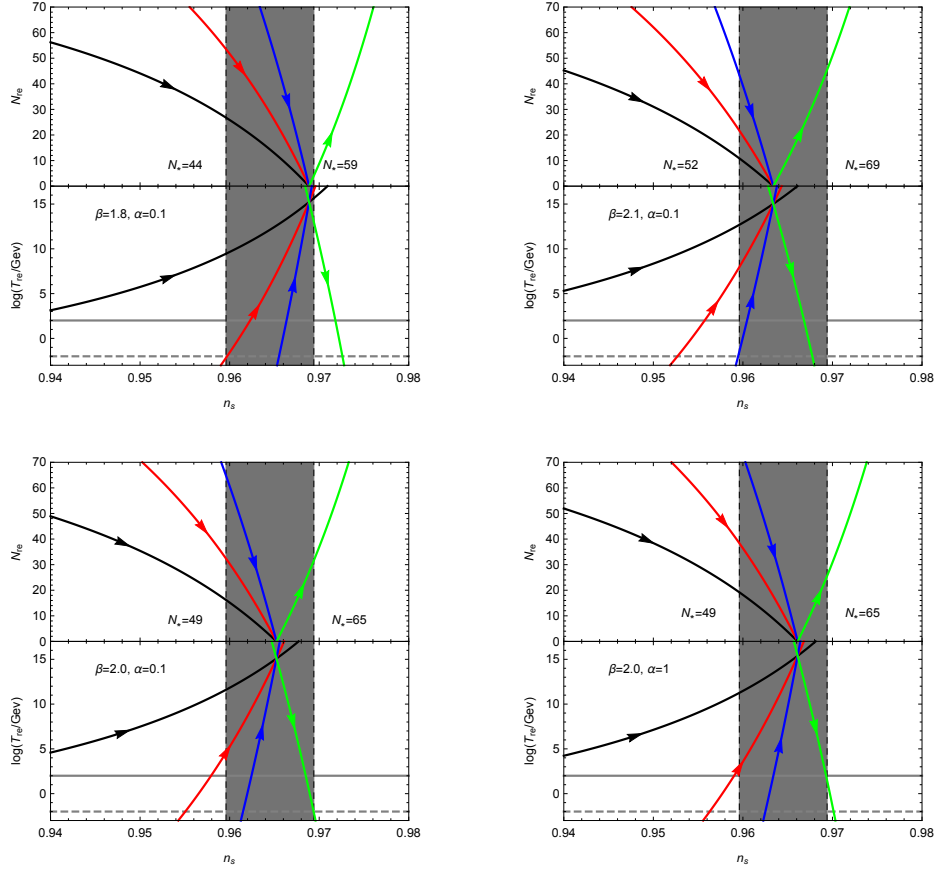


FIG. 8. Same as Fig. 6 but for the model (84), the values of the model parameters  $\alpha$  and  $\beta$  are indicated in each panel.

$\beta(T) = -\sqrt{2}\epsilon$ , so the reconstruction of the tachyon potentials from  $\beta(T)$  is equivalent to the reconstruction from the slow-roll parameter  $\epsilon(T)$  or other parameterizations with the number of  $e$ -folds  $N$ . We focus on the reconstruction of tachyon potentials from the parameterizations with  $N$ .

Following the reconstruction procedure presented in subsection IID, we reconstruct three classes of tachyon potentials by parameterizing the slow-roll parameters  $\epsilon$  (equivalent to the tensor to scalar ratio  $r$ ),  $\eta$  and the observable  $n_s$ , respectively. We first consider the case that the slow-roll parameter is a constant, we find that only the model with  $\eta_V$  being a constant is consistent with the observations at the  $1\sigma$  level, this model is therefore called the constant slow-roll inflation. For  $N_* = 60$ , we get  $-0.0374 < \eta_V < -0.0142$  at the  $1\sigma$  level,  $-0.0435 < \eta_V < -0.0031$  at the  $2\sigma$  level and  $-0.0473 < \eta_V < 0.0067$  at the  $3\sigma$  level, so the concave potential is favored by the observations at more than  $2\sigma$  level. For the simple

model with  $n_s = 1 - p/(N + A)$ , the potential is either power-law or exponential form. Since the observations constrain  $A < 1$ , so the effect of  $A$  is negligible except setting the boundary  $p = 1 + 2A$  for the parameter  $p$ . The  $\alpha$  attractor is the special case with  $p = 2$  and it is consistent with observations. For the power law parametrization  $r = 16\gamma/(N + \alpha)^\beta$ , we find  $\beta \sim 2$  is favored by the observations. For all three models, if we take  $n_s = 0.968$  and  $r = 0.22$ , the reconstructed potentials behave similarly and they are concave potentials.

Depending on the model parameters and the value of  $w_{re}$ , the constraints on  $N_{re}$  and  $T_{re}$  are different, although the parameter  $A$  in the model (67) and the parameter  $\alpha$  in the model (84) have little impact on the reheating phase. For all three models, if we choose the model parameters so that  $n_s$  is consistent with the observations, then reheating with  $-1/3 \leq w_{re} \leq 2/3$  are all consistent with the observations. Furthermore, as  $n_s$  increases, the allowed reheating epoch becomes longer for  $w_{re} = -1/3, 0$  and  $1/6$  while the allowed reheating epoch becomes shorter for  $w_{re} = 2/3$ .

In summary, the main results are: (1) We derive the lower bound on the field excursion for the tachyon inflation, which is determined by the amplitude of the scalar perturbation  $A_s$  and  $N_*$ . The bound is supported by all three models discussed. (2) For the models with constant slow-roll parameter, only the model with  $\eta_V$  being a constant is consistent with the observations at the  $1\sigma$  level and concave potentials are favored by the observations. (3) As  $n_s$  increases, the allowed reheating epoch becomes longer for  $w_{re} = -1/3, 0$  and  $1/6$  while the allowed reheating epoch becomes shorter for  $w_{re} = 2/3$ .

## ACKNOWLEDGMENTS

This research was supported in part by the National Natural Science Foundation of China under Grant No. 11475065 and the Major Program of the National Natural Science Foundation of China under Grant No. 11690021.

- 
- [1] A. Sen, *Rolling tachyon*, *JHEP* **0204** (2002) 048, [[hep-th/0203211](#)].
  - [2] A. Sen, *Tachyon matter*, *JHEP* **0207** (2002) 065, [[hep-th/0203265](#)].
  - [3] G. W. Gibbons, *Cosmological evolution of the rolling tachyon*, *Phys. Lett. B* **537** (2002) 1–4, [[hep-th/0204008](#)].

- [4] T. Padmanabhan, *Accelerated expansion of the universe driven by tachyonic matter*, *Phys. Rev. D* **66** (2002) 021301, [[hep-th/0204150](#)].
- [5] J. Garriga and V. F. Mukhanov, *Perturbations in k-inflation*, *Phys. Lett. B* **458** (1999) 219–225, [[hep-th/9904176](#)].
- [6] J.-c. Hwang and H. Noh, *Cosmological perturbations in a generalized gravity including tachyonic condensation*, *Phys. Rev. D* **66** (2002) 084009, [[hep-th/0206100](#)].
- [7] D. A. Steer and F. Vernizzi, *Tachyon inflation: Tests and comparison with single scalar field inflation*, *Phys. Rev. D* **70** (2004) 043527, [[hep-th/0310139](#)].
- [8] A. D. Linde, *Chaotic Inflation*, *Phys. Lett. B* **129** (1983) 177–181.
- [9] A. A. Starobinsky, *A New Type of Isotropic Cosmological Models Without Singularity*, *Phys. Lett. B.* **91** (1980) 99–102.
- [10] PLANCK collaboration, P. A. R. Ade et al., *Planck 2015 results. XX. Constraints on inflation*, *Astron. Astrophys.* **594** (2016) A20, [[1502.02114](#)].
- [11] Q.-G. Huang, *Constraints on the spectral index for the inflation models in string landscape*, *Phys. Rev. D* **76** (2007) 061303, [[0706.2215](#)].
- [12] R. Gobbetti, E. Pajer and D. Roest, *On the Three Primordial Numbers*, *JCAP* **1509** (2015) 058, [[1505.00968](#)].
- [13] V. Mukhanov, *Quantum Cosmological Perturbations: Predictions and Observations*, *Eur. Phys. J. C* **73** (2013) 2486, [[1303.3925](#)].
- [14] D. Roest, *Universality classes of inflation*, *JCAP* **1401** (2014) 007, [[1309.1285](#)].
- [15] J. Garcia-Bellido and D. Roest, *Large- $N$  running of the spectral index of inflation*, *Phys. Rev. D* **89** (2014) 103527, [[1402.2059](#)].
- [16] J. Garcia-Bellido, D. Roest, M. Scalisi and I. Zavala, *Lyth bound of inflation with a tilt*, *Phys. Rev. D* **90** (2014) 123539, [[1408.6839](#)].
- [17] J. Garcia-Bellido, D. Roest, M. Scalisi and I. Zavala, *Can CMB data constrain the inflationary field range?*, *JCAP* **1409** (2014) 006, [[1405.7399](#)].
- [18] P. Creminelli, S. Dubovsky, D. Lpez Nacir, M. Simonovi, G. Trevisan, G. Villadoro et al., *Implications of the scalar tilt for the tensor-to-scalar ratio*, *Phys. Rev. D* **92** (2015) 123528, [[1412.0678](#)].
- [19] L. Boubekur, E. Giusarma, O. Mena and H. Ramírez, *Phenomenological approaches of inflation and their equivalence*, *Phys. Rev. D* **91** (2015) 083006, [[1411.7237](#)].

- [20] L. Barranco, L. Boubekeur and O. Mena, *A model-independent fit to Planck and BICEP2 data*, *Phys. Rev. D* **90** (2014) 063007, [1405.7188].
- [21] M. Galante, R. Kallosh, A. Linde and D. Roest, *Unity of Cosmological Inflation Attractors*, *Phys. Rev. Lett.* **114** (2015) 141302, [1412.3797].
- [22] T. Chiba, *Reconstructing the inflaton potential from the spectral index*, *Prog. Theor. Exp. Phys.* **2015** (2015) 073E02, [1504.07692].
- [23] F. Cicciarella and M. Pieroni, *Universality for quintessence*, 1611.10074.
- [24] J. Lin, Q. Gao and Y. Gong, *The model independent reconstruction of inflationary potentials*, *Mon. Not. Roy. Astron. Soc.* **459** (2016) 4029–4037, [1508.07145].
- [25] S. Nojiri and S. D. Odintsov, *Unified cosmic history in modified gravity: from  $F(R)$  theory to Lorentz non-invariant models*, *Phys. Rept.* **505** (2011) 59–144, [1011.0544].
- [26] S. D. Odintsov and V. K. Oikonomou, *Inflationary  $\alpha$ -attractors from  $F(R)$  gravity*, *Phys. Rev. D* **94** (2016) 124026, [1612.01126].
- [27] Z. Yi and Y. Gong, *Nonminimal coupling and inflationary attractors*, *Phys. Rev. D* **94** (2016) 103527, [1608.05922].
- [28] S. D. Odintsov and V. K. Oikonomou, *Inflation with a Smooth Constant-Roll to Constant-Roll Era Transition*, 1704.02931.
- [29] S. Nojiri, S. D. Odintsov and V. K. Oikonomou, *Constant-roll Inflation in  $F(R)$  Gravity*, 1704.05945.
- [30] S. Choudhury, *COSMOS- $e'$ - soft Higgsotic attractors*, 1703.01750.
- [31] Q. Gao and Y. Gong, *Reconstruction of extended inflationary potentials for attractors*, 1703.02220.
- [32] R. Jinno and K. Kaneta, *Hillclimbing inflation*, 1703.09020.
- [33] Q. Gao, *The constant slow-roll inflationary model*, 1704.08559.
- [34] N. Barbosa-Cendejas, J. De-Santiago, G. German, J. C. Hidalgo and R. R. Mora-Luna, *Tachyon inflation in the Large- $N$  formalism*, *JCAP* **1511** (2015) 020, [1506.09172].
- [35] L. Dai, M. Kamionkowski and J. Wang, *Reheating constraints to inflationary models*, *Phys. Rev. Lett.* **113** (2014) 041302, [1404.6704].
- [36] J. L. Cook, E. Dimastrogiovanni, D. A. Easson and L. M. Krauss, *Reheating predictions in single field inflation*, *JCAP* **1504** (2015) 047, [1502.04673].
- [37] Y. Ueno and K. Yamamoto, *Constraints on  $\alpha$ -attractor inflation and reheating*, *Phys. Rev. D*

- 93** (2016) 083524, [1602.07427].
- [38] R. Kabir, A. Mukherjee and D. Lohiya, *Reheating constraints on Kähler Moduli Inflation*, **1609.09243**.
- [39] A. Di Marco, P. Cabella and N. Vittorio, *Reconstruction of  $\alpha$ -attractor supergravity models of inflation*, *Phys. Rev. D* **95** (2017) 023516, [1703.06472].
- [40] K. Dimopoulos and C. Owen, *Quintessential Inflation with  $\alpha$ -attractors*, **1703.00305**.
- [41] R. L. Arnowitt, S. Deser and C. W. Misner, *Dynamical Structure and Definition of Energy in General Relativity*, *Phys. Rev.* **116** (1959) 1322–1330.
- [42] D. J. Schwarz, C. A. Terrero-Escalante and A. A. Garcia, *Higher order corrections to primordial spectra from cosmological inflation*, *Phys. Lett. B* **517** (2001) 243–249, [astro-ph/0106020].
- [43] D. H. Lyth, *What would we learn by detecting a gravitational wave signal in the cosmic microwave background anisotropy?*, *Phys. Rev. Lett.* **78** (1997) 1861–1863, [hep-ph/9606387].
- [44] Q. Gao, Y. Gong and T. Li, *Modified Lyth bound and implications of BICEP2 results*, *Phys. Rev. D* **91** (2015) 063509, [1405.6451].
- [45] P. Binétruy, E. Kiritsis, J. Mabillard, M. Pieroni and C. Rosset, *Universality classes for models of inflation*, *JCAP* **1504** (2015) 033, [1407.0820].
- [46] M. Pieroni,  *$\beta$ -function formalism for inflationary models with a non minimal coupling with gravity*, *JCAP* **1602** (2016) 012, [1510.03691].
- [47] P. Binétruy, J. Mabillard and M. Pieroni, *Universality in generalized models of inflation*, *JCAP* **1703** (2017) 060, [1611.07019].
- [48] P. Brax, J. Mourad and D. A. Steer, *Tachyon kinks on nonBPS D-branes*, *Phys. Lett. B* **575** (2003) 115–125, [hep-th/0304197].
- [49] L. R. W. Abramo and F. Finelli, *Cosmological dynamics of the tachyon with an inverse power-law potential*, *Phys. Lett. B* **575** (2003) 165–171, [astro-ph/0307208].